DESTABILIZING EFFECT OF HEAT ON COHERENT STRUCTURES

R.N. Kieft, C.C.M. Rindt and A.A. van Steenhoven
Faculty of Mechanical Engineering
Eindhoven University of Technology
P.O. Box 513, 5600 MB Eindhoven, the Netherlands

ABSTRACT

The effect of heat on coherent vortex structures shed from a cylinder is investigated numerically and experimentally for $Re_D \approx 75$ and $Ri_D = 0 - 1.2$. For the experimental investigation a High Resolution Particle Velocimetry (Hi-Res PV) method is used. For the numerical investigation a Spectral Element Method is used. Both investigations show that for relatively small heat input ($Ri_D < 1$) the vortex street deflects in the direction of the gravity force. Besides, subsequently shed structures show a relative rotation around each other, causing an unstable vortex street. For higher heat input the vortex structures itself become unstable . Three-dimensional structures are formed inside vortices shed from the upper half of the cylinder, occasionally leading to an early breakdown of the vortex street.

1. INTRODUCTION

Coherent structures have a strong influence on the mixing behavior in flow fields. When scalar quantities as mass and heat are captured, for example during the formation process of such a structure, only diffusion processes or strong interactions between the structures can cause any transfer with the surrounding. The effect of this minor mixing behavior can be found in various flow situations. For example in small heat exchangers and electronic devices where the Reynolds number based on the cooling flow is relatively small, coherent structures are formed behind the components to be cooled. These structures which contain relatively warm fluid, will have their influence on the heat transfer of downstream positioned components.

A better understanding of the stability of these structures will lead to a better insight in the mixing behavior of these structures with the surrounding. Especially if these structures become unstable and disintegrate, an improvement of the mixing is obtained. One of the factors which can influence this stability is the scalar quantity which is contained by the structure. For non-passive quantities as temperature, the interaction of the quantity with the momentum conservation relations can influence the stability of the structure and stimulates an early collapse.

The whole process of structure generation and evolution in which the temperature as non passive scalar influences the structure stability is investigated for the horizontal flow around a heated cylinder. The effect of heat on the wake behavior is already investigated for a heated cylinder in an upward vertical flow. Both the numerical results (Noto and Matsumoto (1987)) and experimental results (Michaux-Leblond and Bélorgey (1997)) showed that the generation of vortex structures can be suppressed by increasing the cylinder wall temperature. For the situation where the gravity force and the main flow direction are not along the same axis, less results are presented in literature. Only few results deal about the influence of the main flow attack angle but they have not gone in detail about its effect on the vortices and vortex street stability.

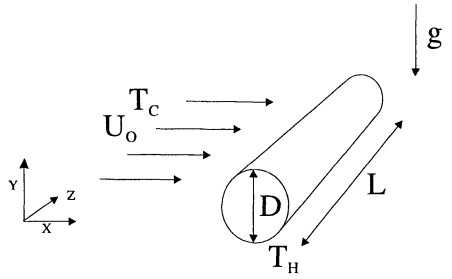

Figure 1: Problem definition

In our investigation a cylinder with diameter D is brought to a temperature T_H and is cooled by a horizontal cross flow U_0 with temperature T_c. The relevant dimensionless parameters are the Reynolds number $Re_D = \frac{U_0 D}{\nu}$, the Richardson number $Ri_D = \frac{Gr_D}{Re_D^2} = \frac{\beta g \Delta T D}{U_0^2}$ and the Prandtl number $Pr = \frac{\nu}{\alpha}$. Here β denotes the expansion coefficient, ν the kinematic viscosity, g the gravity constant, ΔT the temperature difference $T_H - T_c$ and α the thermal diffusity.

The Re_D number in this investigation is chosen to be 75, resulting in the formation of coherent vortex structures which form a stable vortex street for $Ri_D = 0$. Visualization results have shown that by increasing ΔT (or Ri_D) the vortex street and also the vortex structures become unstable, finally leading to an early breakdown of the vortex structures (Kieft *et al.* (1997)). The influence of heat on the vortex structures and the

process which lead to the early breakdown of them will be the main topic of this article. Both numerical and experimental results will be used to elucidate the temperature influence. The first part of the paper therefore briefly describes the used experimental device and method as well as the numerical method. In the remainder the results and the conclusions will be presented.

2. EXPERIMENTAL METHOD

2.1. Test rig

For the experiments a water tank facility is designed in which the heated cylinder ($D = 8.5\,mm$, $L = 495\,mm$) is towed through the motionless tank rather than being exposed to a forced main flow. The specific dimensions of the water tank are for the $length \times width \times height = 500\,cm \times 50\,cm \times 75\,cm$ (Fig. 2).

The main advantage of this device is a minimal creation of boundary layers and an almost uniform inflow velocity distribution (Anagnostopoulos and Gerrard (1978)). Of course the

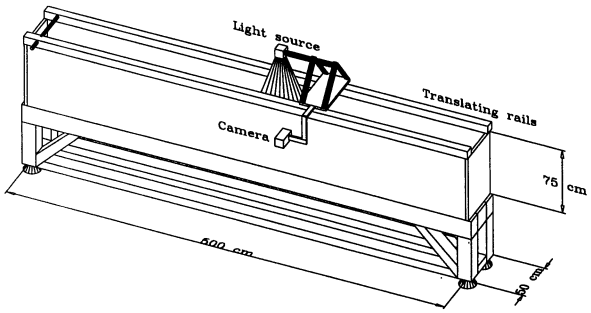

Figure 2: Measuring device

disadvantages of such a device are the occurrence of mechanical vibrations during the translation of the cylinder and the occurrence of background velocities caused by slow thermal convection cells due to temperature differences. The vibrations turned out to be of no significant influence on the fluid motion while the thermal background velocity remains within a few percent of the main flow velocity (Kieft *et al.* (1998)).

To obtain the desired cylinder wall temperature an electric rod heater is used with a maximum heat density of $8.0\,W/cm^2$. The temperature of the cylinder is kept constant in time by controlling the heat input with the help of the measured wall temperature.

The translation of the construction is obtained by an electric motor which is corrected for its variation in rotational speed by means of a closed circuit, resulting in a variation in the rotational speed of less than 0.2 percent. The motor is coupled to the drive wheel by using a $1 : 100$ gear. Around the drive and the idle wheel of the translation system an almost inelastic fiber based tape is looped which is finally connected to the camera/cylinder construction.

2.2. Particle Tracking

The structures inside the cylinder wake are measured with help of a High Resolution Particle Velocimetry method (HiRes-PV). This method, which is a combination of Particle Tracking Velocimetry (PTV) and Particle Image Velocimetry (PIV) (van der Plas and Bastiaans (1998)), is capable of tracking about 6000 till 8000 vectors inside a plane of the flow domain (fig 3). This high spatial resolution makes it possible to calculate very accurately structure characteristics as strength and centroids, two quantities which will be used in the investigation of heat induced effects on the stability of the structures.

In this combined method, PIV is used as a preprocessing for the Particle Tracking (PT) algorithm. Within the PT algorithm the measured PIV velocity is used as initial guess for the new position of a particle in a frame $t + \Delta t$. This allows to do particle tracking in a domain where the seeding density is much higher than the maximum seeding density for just single PTV.

The seeding used are 10 and 20 μm hollow glass particles which are illuminated with a 200 mJ pulsed Nd:YAG laser. The recording is done by a 1024^2 high resolution 30 Hz Kodak ES1.0 monochrome camera which is directly coupled to the data acquisition system. The data is processed off line with the own made HiRES-PV code (van der Plas and Bastiaans (1998)). The results of this code are tracked particle paths which can be used for the calculation of the vector field. The vectors are calculated by an algorithm which uses only particles which can be found in at least five subsequent video frames.

Vectors which show a too strong variation with respect to their surrounding are removed by statistical considerations. The obtained vector field is unstructured which makes it more

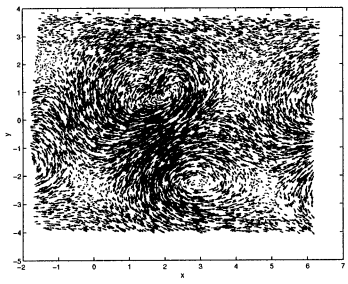

Figure 3: Unstructured vector field

difficult to calculate derived quantities as vorticity and vortex strength. Structured data points are calculated from the PTV data field by using a Gaussian weighting function. If proper parameters are used during this interpolation, no crucial information is lost (Agui and Jimenez (1987)).

3. NUMERICAL METHOD

In order to investigate the effect of the induced heat on the vortex shedding process a 2-D spectral element code is developed. The basic ideas of the developed code will be briefly described below, a more thorough description can be found in Timmermans (1994) and Canuto *et al.* (1988).

3.1. Temporal discretization

Solving the relevant instationary equations for mass, momentum and heat two major problems have to be overcome. The first problem concerns the presence of both a convection and a diffusion part in the conservation equations for energy and momentum. For spectral methods the eigenvalues of the diffusion matrix are negative and real, while the eigenvalues for the convection matrix are imaginary with a small negative real part (Canuto *et al.* (1988)). Besides, the convection matrix is time dependent. A direct discretization of the convection/diffusion equation is therefore not an effective approach. Within this code an operator splitting method is used. Here the combined diffusion-convection equation is split into a diffusion and a convection equation (Minev *et al.* (1996)). The convection problem is discretized by applying a three steps explicit Runge-Kutta scheme while the diffusion equation is discretized by a third order backward difference scheme.

The second problem is related to the incorporation of the incompressibility constraint and calculation of the pressure. This is done by means of a pressure correction method (Timmermans *et al.* (1996)). Here the pressure and velocity are decoupled by first making a prediction of the pressure on time level $n+1$ for a prediction velocity at $n+1$. Secondly, this velocity will be corrected in such a way that the incompressibility constraint will hold again.

3.2. Spatial discretization

Spatial discretization is obtained by using a Spectral Element approach. The variational formulation is used as a basis for the discretization process, leading to a Galerkin weighted residual approach (Patera (1984)). Here the domain is divided into several spectral elements on which the variables are approximated by high order polynomial expansions. As a general form of the applied polynomial expansion for the unknown u we state

$$u(x) = \sum_{i=0}^{n} u_i \phi_i(x) \,, \tag{1}$$

with $u_i = u(x_i)$. The basis function is chosen to be

$$\phi_i^n(\xi_j) = -\frac{1}{n(n+1)L_n(\xi_i)} \frac{1-x^2}{x-\xi_i} \frac{dL_n}{dx} \,, \tag{2}$$

with L_n the n^{th} order Legendre polynomial. In order to define an n^{th} order polynomial on each sub domain one has to introduce internal points. One can prove (Patera (1984)) that if Gauss-Lobatto points are used as internal points spectral convergence is obtained.

4. RESULTS

First the behavior of the vortex structures inside the wake is examined. This is done by tracing the shed vortex structures during there downstream convection. The camera is then fixed to the carrying construction and focusing on a domain just behind the cylinder (typically $0 < x < 25D, -8D < y < 8D$) where the cylinder is positioned in $x/D = 0$, $y/D = 0$. Within this window the positions of the vortices are determined from the measured vorticity field which shows clearly peaks and dips within the interrogation area. The structure position (X, Y) and its strength Γ is then determined by

$$X = \int_A \omega_z(x,y) x dA/\Gamma \tag{3}$$

$$Y = \int_A \omega_z(x,y) y dA/\Gamma \tag{4}$$

$$\Gamma = \int_A \omega_z(x,y) dA. \tag{5}$$

with ω_z the out of plane component of the vorticity vector, the only vorticity component occurring for a 2D flow. The area A is defined as the area enclosed by the iso-vorticity contour $\omega = 0.2$.

For every calculated vorticity field, the shed structures are detected. During the experiment (which takes about 120 sec.) those detected structures are tracked. By plotting the average structure trajectories the influence of heat on the cylinder wake becomes clear. For relatively low heat input ($Ri_D = 0-1$) the vortex street is deflected in the direction of the gravity force. This unexpected behavior is both measured (fig. 4) and numerically calculated (fig. 5), where the main discrepancy between the numerical and experimental results is the wake behavior for $Ri_D = 0.5$. The numerical results show that the strongest deflection occurs for $Ri_D = 0.5$ while in the experimental results for $Ri_D = 1$ the strongest deflection occurs. This difference might be caused by the unavoidable presence of large scale background fluid motions (see section 2.1).

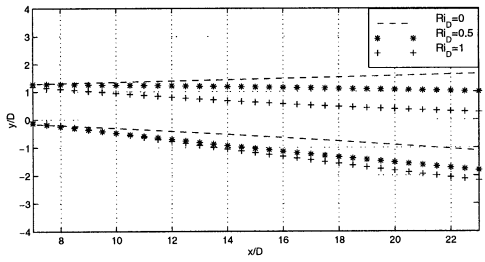

Figure 4: Experimental trajectories

Considering the effect of heat on the momentum equation the deflection is a remarkable behavior which can be explained by considering the strength of the vortex structures. Their strength shows an asymmetry between the strength of a negative structure (shed from the upper half of the cylinder) and a positive structure (shed from the lower half). Both measurements as well as the calculations show that the upper vortices are about 20 percent stronger than the lower vortices. This strength difference causes the deflection of the vortex street which can be explained by a point vortex consideration. The stronger upper vortices first cause the lower vortex to move slower downstream than the upper vortices, resulting

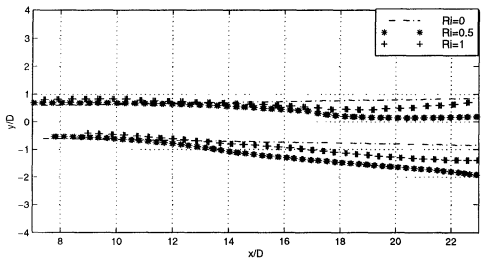

Figure 5: Numerical trajectories

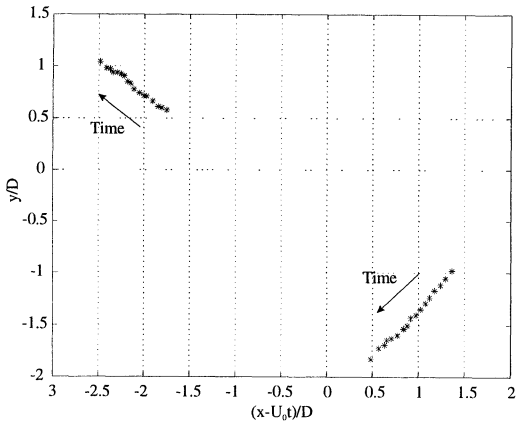

Figure 6: Experimental trajectories of two subsequently shed vortex structures for $Ri_D = 0$,the cylinder position at $t = 0$ was ($x_0 = -3.5D$, $y_0 = -0.3D$)

in a disturbed vortex street. While in the undisturbed vortex street configuration the y-velocity induced by the structures is canceled out, in this disturbed situation a net y-velocity occurs (Kieft *et al.* (1998)) which causes the deflection.

Besides the deflection of the vortex street, the street it self becomes also unstable by this strength difference. For $Ri_D = 0$ the structures within the vortex street are positioned on an almost stationary position with respect to each other, for $Ri_D > 0$ a relative movement of the structures occurs. This relative movement is examined by considering the behavior of two subsequently shed vortex structures. In contrast to the experiments which were done to examine the wake behavior, now the camera is decoupled from the carrying construction and placed on a fixed position. The structures which are shed from the cylinder remain within the interrogation area at which the camera is focussed. So it is now possible to evaluate for a long time the evolution of a shed structure. By plotting the found structure positions (centroids) for about 40 s, one can observe the relative movement between two subsequently shed structures. The position of the shed structure with respect to the position of the cylinder x, can easily be calculated by using the velocity of the cylinder ($U_0 = 8.5\, mm/s$) and its position x_0, y_0 at $t = 0s$.

For $Ri_D = 0$ (fig. 6) it can be seen that both the upper and lower vortices move in the direction of the cylinder. This movement can be understood by examining a point vortex representation from which it is found that the vortex structures induce a velocity on each other. Also a movement in y-direction can be observed. This movement is likely to be caused by diffusion processes in the vortex structures resulting in a widening of the vortex street (this can also be seen in fig. 4 and 5). Only the movement in y-direction causes a small relative movement between the structures. However the configuration of the vortex street remains almost preserved (fig. 6).

For $Ri_D = 0.5$ still both vortices move in the direction of the cylinder (negative x direction), but the lower vortex moves much faster (fig. 7). Besides, during the experiment both structures are moving in negative y-direction resulting in the deflection of the vortex street. By concerning the relative distance between the two vortices, one can see that the lower vortex seems to rotate around the upper vortex. The presence of this strong relative movement between the structures shows that the vortex street is not a stable configuration of vortices anymore, resulting in an unstable vortex street. The source of this relative movement, as explained before, turns out to be the strength differences between the structures in the upper vortex and lower vortex row.

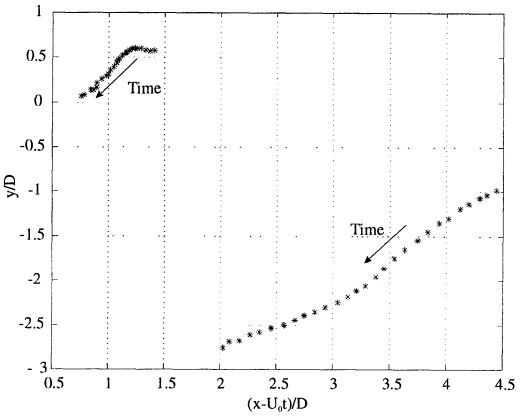

Figure 7: Experimental trajectories of two subsequently shed vortex structures for $Ri_D = 0.5$, the cylinder position at $t = 0$ was $x_0 = D$, $y_0 = -0.3$

A similar behavior can be found for $Ri_D = 1$, where the rotation is even more severe. Here the rotation causes a situation where the lower vortex structures has over taken the upper one (fig. 8,), a very unstable situation considering the vortex street stability.

For $Ri_D > 1$ (fig. 9) the evolution of the structures shows in the first part of the experiments a similar behavior as for $Ri_D < 1$. Also a relative movement of the lower around the upper vortex occurs, only this movement is stronger, and the unstable situation as described before occurs earlier. Further-

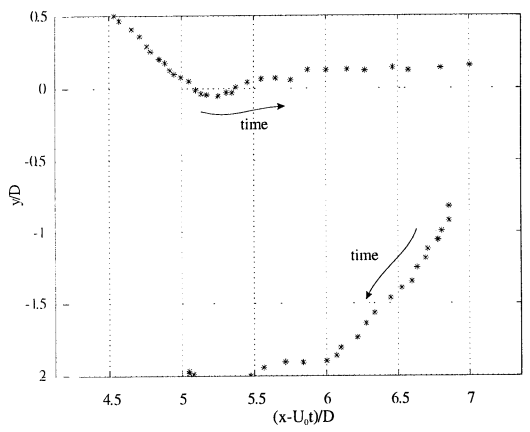

Figure 8: Experimental trajectories of two subsequently shed vortex structures for $Ri_D = 1$, the cylinder position at $t = 0$ was $x_0 = 3D$, $y_0 = -0.3D$

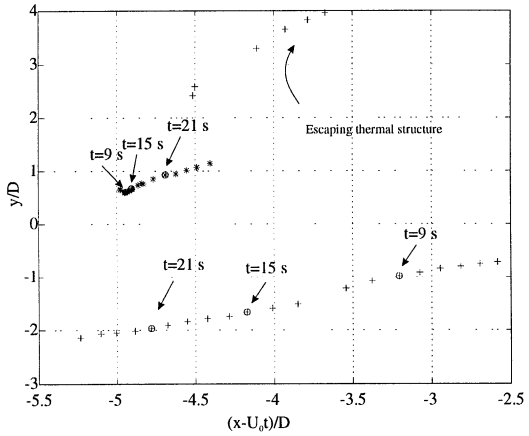

Figure 9: Experimental trajectories of two subsequently shed vortex structures for $Ri_D = 1.2$. The + marks denote the positions of positive structures, the * the positions of negative ones, the position of the cylinder at $t = 0$ was $x_0 = -7.5D$, $y_0 = -0.3D$

more, the upper vortex moves continuously upward while the vertical movement of the lower vortex is less negative. This means that the negative deflection of the vortex street does almost not occur anymore, indicating that the vortex strength induced behavior is over taken by the heat induced mechanism which causes an upward flow.

Figure 9 also shows an additional path formed by a structure with positive circulation (+ marks). This trajectory is elucidated by the vorticity distribution plots (fig. 10) which show the evolution of two subsequently shed structures after the moment that the cylinder is towed through the test domain (at $t = 0s$ the cylinder was positioned at $x \approx -7$ and $y = 0$). During the evolution for $Ri_D > 1$ it can be seen in the vorticity plots (fig. 10) that inside a negative vortex structure a patch of positive vorticity is growing (fig. 10a-b). First the vortex structure transforms in a kidney shaped structure in which an area of positive vorticity is growing (fig. 10b) . In combination with the negative vorticity from the original structure, a kind of dipole structure is formed (fig. 10c). This dipole structure escapes from the original structure, leaving behind a trail of negative vorticity. The positive part can also be found back in the calculated vortex positions (fig.9) where a path can be seen starting at $x = -4.5D$, $y = 2.5D$).

After the escape of the dipole structure, the vorticity distribution becomes irregular indicating that the coherent structures has fallen apart. In other words, the coherent structures which can be found for $Ri_D = 0$ disintegrate for $Ri_D > 1$ resulting in an early break down of the vortex street.

This process of a growing positive vorticity patch can also be seen in the numerically calculated vorticity plots (fig. 11). Again the transformation of the shed structure into a kidney shaped structure can be observed. Although the initiation process of the dipole shaped structure is occurring, no escape of it can be observed. This is probably a 3D effect.

5. Discussion and conclusions

For relatively low Ri_D numbers the effect of heat on the vortex street is a deflection of the vortex street in the direction of gravity force. This remarkable behavior is caused by a strength difference between the upper and lower vortices which is both observed in the numerical and the experimental results.

Besides this deflection, the strength difference causes also an instationary behavior of the vortex structures within the vortex street. A relative movement of two subsequently shed structures is observed for $Ri_D > 0$ where a lower vortex rotates around a sequently shed upper vortex. The strong linking which occurs between the shed structures in the original vortex street is now entirely damaged. This results in a very unstable vortex street situation.

For $Ri_D > 1$ the vortex structures itself become unstable during the experiments (the interrogation time was maximum 45 seconds). The process leading to the occurrence of an unstable vortex structure starts with the deformation of a shed negative structure into a kidney shaped structure. Within this kidney shape, an area of positive vorticity is developing. As soon as this structure reaches a certain strength or size it forms together with negative vorticity from the environment, a dipole like structure. This dipole accelerates and escapes from the vortex street.

Up to a certain point the process as described above, can be observed in the numerical results. Only the formation of the dipole shaped structure and its escape can not be simulated. The 2D numerical code is not capable of representing this process, allowing us to think that the latter process might be a 3D process. The 3D character of the escaping structure is also verified by earlier published visualization results (Kieft *et al.* (1997). In the near future, the whole process of wake

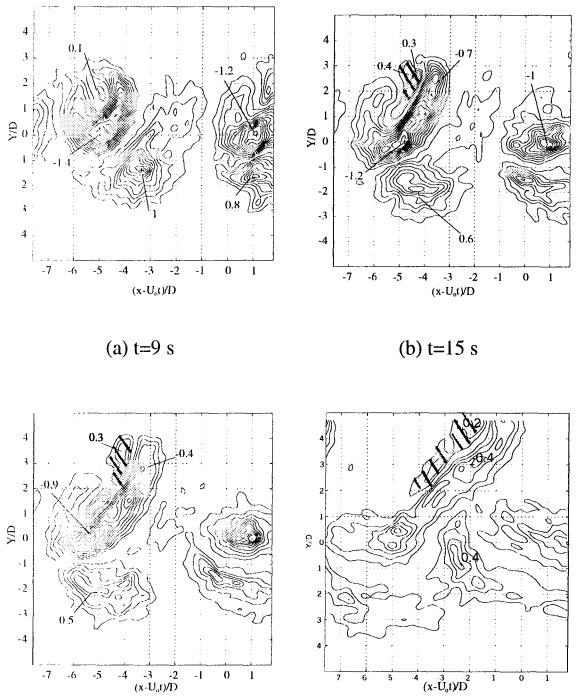

(a) t=9 s (b) t=15 s

(c) t=21s (d) t=33 s

Figure 10: Evolution of the shed vortex structures for $Ri_D = 1.2$, the area of positive growing vorticity is marked

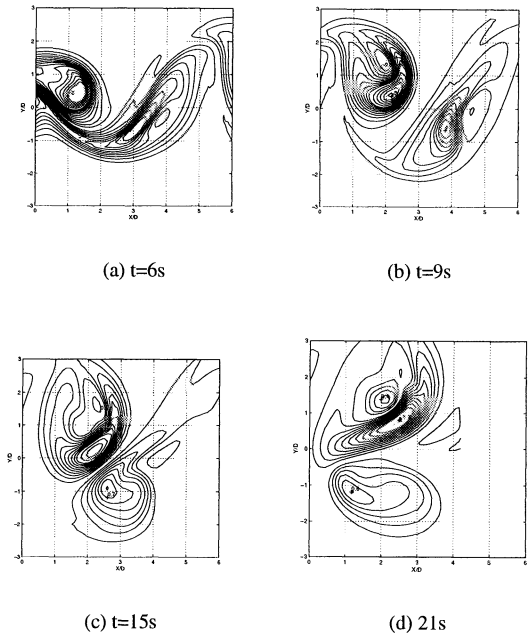

(a) t=6s (b) t=9s

(c) t=15s (d) 21s

Figure 11: Evolution of the shed vortex structures for $Ri_D = 1.2$, the cylinder position at $t = 0$ was $x_D = 0$, $y_D = 0$

transition will be investigated by 3D simulations and 3D experiments.

References

Agui, C. and Jimenez, J. (1987). On the performance of Particle Tracking. *Journal of Fluid Mechanics*, **185**, 447–468.

Anagnostopoulos, E. and Gerrard, J. (1978). A towing tank with minimal background motion. *Journal of Physics E*, **9**, 951–954.

Canuto, C., Hussaini, M., Quarteroni, A., and Zang, T. (1988). *Spectral Methods in Fluid Dynamics*, chapter 13. Springer Verlag.

Kieft, R., Rindt, C., and van Steenhoven, A. (1997). Mixed convection around a heated cylinder. In *Turbulence Heat and Mass Transfer 2*, pages 85–94. Delft University Press.

Kieft, R., Rindt, C., and van Steenhoven, A. (1998). The influence of buoyancy on the behavior of the vortex structures in a cylinder wake. In *Proceedings of the 11th International Heat and Mass Transfer Conference, Kyongju, Korea*, volume 3, pages 219–225.

Michaux-Leblond, N. and Bélorgey, M. (1997). Near-wake behavior of a heated circular cylinder: viscosity-buoyancy duality. *Experimental Thermal and Fluid Science*, **15**, 91–100.

Minev, P., van der Vosse, F., Timmermans, L., and van Steenhoven, A. (1996). A second order splitting algorithm for thermally-driven flow problems. *Int. J. Num. Meth. Heat Fluid Flow*, **6**, 51–60.

Noto, K. and Matsumoto, R. (1987). Numerical simulation on the development of the Karman vortex street due to the negatively buoyant force. In *Numerical methods in laminar flow, 5th conference*, pages 796–809.

Patera, A. (1984). A spectral element method for fluid dynamics: laminar flow in a channel expansion. *Journal of Computational Physics*, **54**, 468–488.

Timmermans, L. (1994). *Analysis of spectral element methods*. Ph.D. thesis, Eindhoven University of Technology, Department of Mechanical Engineering.

Timmermans, L., Minev, P., and van de Vosse, F. (1996). An approximate projection scheme for incompressible flow using spectral elements. *Int. J. Num.Meth. in Fluids*, **22**, 673–688.

van der Plas, G. and Bastiaans, R. (1998). Accuracy and resolution of a fast ptv-algorithm suitable for hires-pv. In *Prodeedings of the 8th International Symposium on Flow Visualisation*, paper no. 87.